Aerosol and Air Quality Research, 18: 2967–2981, 2018

ISSN: 1680-8584 print / 2071-1409 online
doi: 10.4209/aaqr.2018.04.0129

Characterization of PM_1-Bound Metallic Elements in the Ambient Air at a High Mountain Site in Northern China

Jun-Jie Yue[1], Roberta Palmiero[1,2], Yang-Yang Han[3], Yan Wang[4], Qian-Qian Li[5], Tuo-Yu Zhang[3], Meiqing Sun[6], Hong Wang[6], Guangping Yu[6], Xian-Liang Yi[7], Peng-Hui Li[1*], Ya-Qin Ji[8], Li-Qiong Guo[9]**

[1] *School of Environmental Science and Safety Engineering, Tianjin University of Technology, Tianjin 300384, China*
[2] *Department of Civil, Architectural and Environmental Engineering (DICEA), University of Naples Federico II, 80125 Naples, Italy*
[3] *Tianjin Institute of Scientific and Technical Information, Tianjin 300074, China*
[4] *School of Environmental Science and Engineering, Shandong University, Jinan 250100, China*
[5] *Neurology Department, General Hospital of PLA, Beijing 100853, China*
[6] *Wuqing District Center for Disease Control and Prevention, Tianjin 301700, China*
[7] *School of Food and Environment, Dalian University of Technology, Panjin 124221, China*
[8] *College of Environmental Science and Engineering, Nankai University, Tianjin 300071, China*
[9] *Department of Occupational and Environmental Health, School of Public Health, Tianjin Medical University, Tianjin 300070, China*

ABSTRACT

The PM-bound metallic elements in 43 daily PM_1 samples collected at Mount Tai during a summer campaign were analyzed by ICP-MS. The PM_1 concentrations ranged between 11.02 and 83.71 μg m^{-3}, with an average of 38.98 μg m^{-3}, and were influenced by meteorological events, exhibiting an increasing trend in the early stage of rain, followed by a significant decrease denoting efficient scavenging. Higher elemental concentrations were detected at Mount Tai than at other overseas background sites. According to the enrichment factor (EF) and geo-accumulation index (Igeo) calculations, among the 16 considered elements, Mn, Al, Co, Sr, Mo, Fe, Ca, V, Ti and Ni in the PM_1 were mainly of crustal origin, while Cu, Cr, As, Zn, Pb and Cd were primarily due to anthropogenic causes. Source identification via Pearson correlation analysis and principle component analysis showed that coal mining and coal burning activities, metal processing industries and vehicle emissions were common sources of heavy metals on Mount Tai; these results were consistent with the air mass analysis. The estimated hazard indexes for all population groups (the elderly, males, females and children) were smaller than 1, suggesting that non-carcinogenic effects due to heavy metal inhalation were unlikely to occur. However, in the present study, the incremental lifetime cancer risk values were about 10 times higher than the reference value of 1×10^{-6}, indicating a potential health risk to the general population.

Keywords: Submicron particles; Metallic elements; Air transport; Source analysis; Risk assessment.

INTRODUCTION

Metallic elements are among the several components of PM_1 (particulate matter with an aerodynamic diameter of 1 μm or smaller) along with ionic species, carbonaceous species, sulfates, nitrates, chlorides, ammonium and particle-bound water (Harrison *et al.*, 2004; WHO, 2013). They originate from both natural and anthropogenic causes, the latter including combustion processes, traffic emissions, domestic and industrial activities (Huang, 2013; Zhai *et al.*, 2014; Ventura *et al.*, 2017).

Particles carrying metals may have an atmospheric lifetime varying from the order of days to weeks, and they can be easily transported over long distances (Radulescu *et al.*, 2015; Kozakova *et al.*, 2017) before they are removed by wet or dry deposition. The wet deposition mechanism depends on the interaction between hydrometeors (cloud droplets, mist, rain and ice crystals) and particles whose growth determinates deposition on the earth's surface

* Corresponding author.
Tel.: 86 22 60214184
E-mail address: lipenghui406@163.com
** Corresponding author.
Tel.: 86 22 23501512
E-mail address: jiyaqin@nankai.edu.cn

(Blanco-Becerra *et al.*, 2015). The dry deposition refers to other processes such as gravitational settling and capture by obstacles at the ground (Prodi and Tampieri, 1982).

Since atmosphere is one of the major pathways of metal dispersion in the environment (Lin *et al.*, 2016), recent researches have been carried out investigating the pollution characteristics and the anthropogenic sources of PM-bound metallic elements (Papaoikonomou *et al.*, 2018). Submicron particles (PM_1) are of special concern due to their anthropogenic origin and potential to cause cardiorespiratory or carcinogenic diseases (Vecchi *et al.*, 2008; Galindo *et al.*, 2013). According to these results, PM1-bound elemental composition is strictly dependent on the pollution sources where light metals (i.e., Ca, Mg, Al and Na) are primarily from natural sources and heavy metals mainly originate from different anthropogenic sources. In the research conducted in Ulsan, Korea, Cd was more enriched in PM_1 and it originated mainly from vehicle exhaust (Hieu and Lee, 2010). In Algiers, Algeria, Pb was the most abundant among heavy metal compounds (HMs) (Talbi *et al.*, 2018), with an annual average concentration of 200 ng m^{-3} at an urban site caused by vehicle emission. As, Ag and Cd were strongly enriched in PM_1 in Changji, China (Liu *et al.*, 2017b), with mean enrichment factors (EFs) of 485.97, 129.40 and 118.47, respectively, indicating the anthropogenic contribution.

Seasonal variation and long-range transport were other important factors affecting metallic element concentrations. The concentrations of metallic elements are usually higher in winter due to the stability of the atmosphere with low mixing height, the increasing of combustion activities and less atmospheric turbulence (Singh and Gupta, 2016; Majewski *et al.*, 2018). Air masses from heavy polluted regions were responsible for the enrichment of metallic elements in the downwind areas (Galindo *et al.*, 2016).

In comparison to other countries, metallic element pollution in the atmosphere of China is more severe due to rapid urbanization and industrialization (Liu *et al.*, 2017b), and an increasing trend of pollution levels had been reported in recent years (Pacyna and Pacyna, 2001). A few studies have been conducted to assess atmospheric metallic element levels in different geographical areas, and results from these studies indicated that spatial distribution characteristics of metallic element emissions are closely related with the unbalanced regional economic development and population density. For example, coastal regions have been zoned as the most polluted areas by atmospheric HMs in China (Tian *et al.*, 2015). However, little work has been done at regional background sites, and the analysis for atmospheric transport of PM_1-bound metallic element was limited. As such, a monitoring campaign was performed in the summer of 2015 at the summit of Mount Tai. The sampling site served as a regionally representative background site and a unique environment to study the transport of pollutants in the free troposphere (Li *et al.*, 2010, Wang *et al.*, 2011). The objectives of the present study were 1) to measure the concentration of PM_1-bound metallic elements compounds (special for HMs); 2) to evaluate the influence of meteorological parameters on the metallic element levels; 3) to give insights on the regional atmospheric source apportionment of PM_1-bound metallic elements by applying correlation analysis, back-trajectory model and principle component analysis (PCA) and 4) to assess the risk associated with the inhalation exposure for both toxic and carcinogenic HMs.

MATERIALS AND METHODS

Sampling Site

PM_1 samples were collected during a summer campaign (June 22–August 11, 2015), which was conducted at a meteorological station (36.25°N, 117.10°E) set at the summit of Mount Tai (1534 m a.s.l.). Mount Tai (Fig. 1) is located in the north of Tai'an City in the middle of Shandong Province, and it is about 230 km far from the Pacific Ocean. This area is one of the most rapidly developing regions in China and one of the most polluted regions in the world. As the highest point in the North China Plain, the summit of Mount Tai represents a regional background site reflecting the basic pollution status of the free troposphere (Liu *et al.*, 2017a).

PM_1 Collection and Analysis

Forty-three daily PM samples (23 h, from 9 a.m.–8 a.m.) were collected by a low-volume sampler (LVS, manufactured by Comde-Derenda (Wuxi) Measuring Technologies Co., Ltd, Germany), operating at a flow rate of 38 L min^{-1} with a 1-μm cut-point for PM_1. Before sampling, polypropylene membrane filters (φ = 47 mm) were prefired at 60°C for 0.5 h and pre-conditioned at controlled environment condition (relative humidity of 45% and temperature of 22°C) for 48 h (USEPA, 2001). Then they were weighed using a microbalance (balance sensitivity ± 0.001 mg, Mettler Toledo XP6). After sampling, the filters were reconditioned for another 48 h and weighed again. Then they were packed with aluminum foil and stored at –4°C.

The analyses of 27 elements (V, Cr, Mn, Co, Ni, Cu, Zn, As, Cd, Pb, Li, Be, Na, P, K, Sc, Rb, Y, Mo, La, Ce, Sm, W, Tl, Bi, Th, U) were performed on inductively coupled plasma-mass spectroscopy (ICP-MS) (Agilent 7500a, Agilent Co., USA). The analytical protocols strictly followed those described by Li *et al.* (2013). Briefly, each polypropylene membrane filter was cut into 2 pieces and placed in a 100 mL polyfluortetraethylene beaker with 5 mL HNO_3 (pH = 5.6) and a drop of HF (pH = 5.3). After covering the solution, the filter was transferred over a hot plate at 220°C for 2.5 h, then 5 mL hydrochloric acid were added. Deionized water was also added to dilute the digested samples to 10 mL. Simultaneously, national soil reference standard, GBW07402 (GSS-2), was analyzed for quality control. Recoveries of the analytes by the utilized technique were from 80% to 120%. Background contamination was assessed using operational blanks that were processed simultaneously with field samples. 1 standard sample was analyzed per 10 field samples to assure the repeatability of the analytic instrument. 1 field sample was analyzed twice per 10 samples to assure the relative errors were less than 20%.

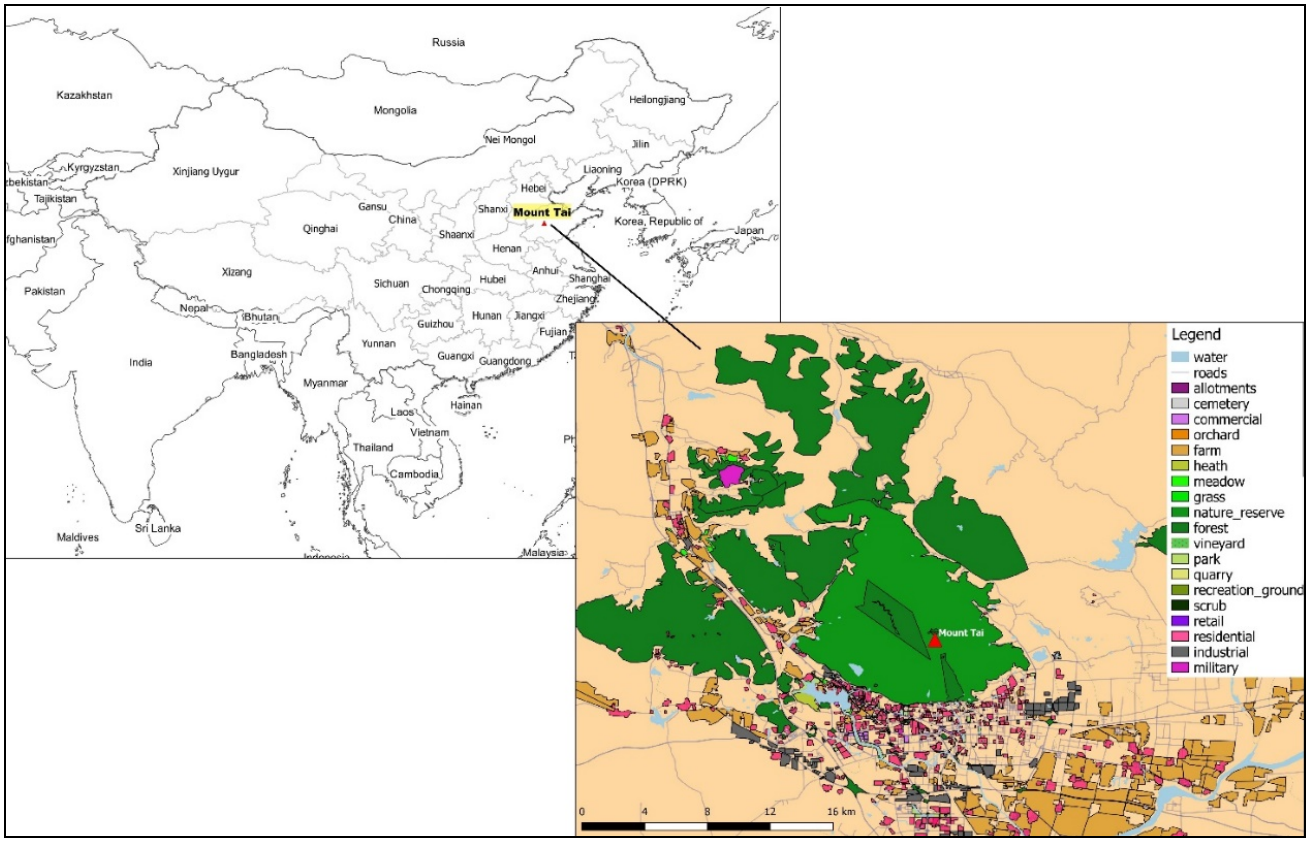

Fig. 1. Location of the sampling site and landcover information about the immediate nearby area of Mount Tai. © OpenStreetMap contributors.

Enrichment Factor (EF) and Geo-Accumulation Index (Igeo)

The enrichment factor (EF) and geo-accumulation index (Igeo) analyses were performed to identify whether the environmental elements were natural or anthropogenic in origin. The EF is based on the normalization of a given metal against a conservative reference element. In this study, EF values were calculated with respect to Al according to Eq. (1):

$$EF = (C_n/C_{ref})_{sample}/(B_n/B_{ref})_{crust} \quad (1)$$

where $(C_n/C_{ref})_{sample}$ and $(B_n/B_{ref})_{crust}$ were the concentration ratios of the target metal to the reference element (Li *et al.*, 2016) in the samples and in the Shandong Province upper crust, respectively. EFs close to 1 pointed to a crustal origin, while those greater than 10 were considered to have a non-crustal source.

The Igeo can be evaluated by Eq. (2):

$$Igeo = \log2(Cn/1.5Bn) \quad (2)$$

Igeo is distinctive from EF since a constant (generally set at 1.5) is introduced to compensate possible variations of the background values that are caused by lithogenic effects (Odat, 2015; Olatunde, 2015).

Principal Component Analysis (PCA)

PCA was conducted in this study for factor reduction. The PCA model extracts a smaller number of uncorrelated components from a large set of variables which explain a maximum of the variance in the data (Khan *et al.*, 2012). The analysis was performed using Statistical Product and Service Solutions software (SPSS v.20). Factors with eigenvalues greater than unity were considered in this study and Varimax normalized rotation was applied to make the results more easily interpretable.

Health Risk Assessment

In this study, a health risk assessment model for inhalatory exposure was applied based on the method developed by the United States Environmental Protection Agency. To calculate the lifetime average daily doses of carcinogens (LADD, mg kg^{-1} d^{-1}) and the average daily doses of non-carcinogens (ADD, mg kg^{-1} d^{-1}), the following equation (Eq. (3)) was used (Liu *et al.*, 2017b):

$$ADD/LADD = (C \times RR \times Ef \times ED)/(BW \times AT) \quad (3)$$

C = Concentration of the contaminant (mg m^{-3});
RR = Respiratory rate (m^3 d^{-1});
Ef = Exposure frequency (d a^{-1});
ED = Exposure duration (a);
BW = Body weight (kg);
AT = Averaging time (d).

Hazard quotients (HQs) were derived for non-carcinogenic metals (Eq. (4)). Hazard indexes (HIs) were also calculated

(Eq. (5)) to evaluate the overall potential non-carcinogenic effects posed by more than one chemical (Zheng *et al.*, 2015). HI larger than 1 indicates a significantly adverse non-carcinogenic effect (Huang *et al.*, 2014). In addition, incremental lifetime cancer risk (ILCR) was calculated (Eq. (6)) for each carcinogenic metal.

$$HQ = ADD/RfD \quad (4)$$

ADD = non-carcinogenic metal dose (mg kg^{-1} d^{-1});
RfD = Reference dose (mg kg^{-1} d^{-1}).

$$HI = \sum HQi \quad (5)$$

$$ILCR = LADD \times SF \quad (6)$$

LADD = carcinogenic metal dose (mg kg^{-1} d^{-1});
SF = slope factor.

RESULTS AND DISCUSSION

PM_1 Characterization

The daily overall concentrations of PM_1 collected on Mount Tai during the sampling period were calculated and the time-series is shown in Fig. 2. The measured PM_1 levels ranged from 11.02 to 83.71 μg m^{-3}, with an average of 38.98 μg m^{-3}. Though aerosol cycles do not necessarily adhere to the workday schedule of humans (Stallins *et al.*, 2013), it was observed that most of the peaks occurred during the weekdays, especially on Mondays and Tuesdays. A similar pattern for PM_1 was observed by Ollier (2013) in a residential area of Zagreb, Croatia, which was attributed to higher traffic pollution in ambient air at the start of the week. A "Monday-effect" was also recorded for $PM_{2.5}$ in a study conducted in urban sites in California (Motallebi *et al.*, 2003). The above mentioned two studies reported that weekend average concentrations were generally lower than the weekday ones, which was due to the decreasing in traffic emission in weekends. In contrast, no significant difference was found for PM_1 concentration between weekdays and weekends in this study because of a diffused background presence and secondary formation of fine particle. It was also suggested the reduced weekend traffic emissions had a lower impact on the concentration levels for the finest PM fractions (Aurela *et al.*, 2015).

Since there is no prescribed standard for PM_1, the concentrations were compared to the WHO 24-h mean limit for $PM_{2.5}$ (25 μg m^{-3}) (WHO, 2006; Křůmal *et al.*, 2017). Most of the measured PM_1 concentration exceeded the standard during the observation campaign. The PM_1 concentrations obtained at Mount Tai were in perfect agreement with results of a previous study carried out in this area in 2014 (Table 1) (Zhao *et al.*, 2017). Besides, the results were also comparable to those reported in Lake Hongze, a national background site in northern China, suggesting relatively background concentrations of northern China. The measured PM_1 concentrations were generally lower than those in Xi'an, China, much higher than the ones observed in the urban areas of Barcelona (Spain), Lucknow (India) and Guangzhou (China), and 3–4 times higher than those measured at Mount Wuzhi in southern China.

The average concentration of the total metallic elements was 9.18 μg m^{-3}, ranging from 2.97 to 38.42 μg m^{-3} (Table 2), accounting for 23.6% of PM_1 mass. Among the detected elements, the most abundant one was Si (range: 0.71–8.54 μg m^{-3}), with an average concentration of 2.43 μg m^{-3}. Fe, Al, Ca, Na, Mg, Ti, K were the next most abundant elements in the PM_1, and together with Si, they accounted for 98.46% of the total elemental concentration (Fig. 3).

Among the elements, seven heavy metal compounds (HMs) (including Pb, V, As, Mn, Ni, Cr and Cd) were

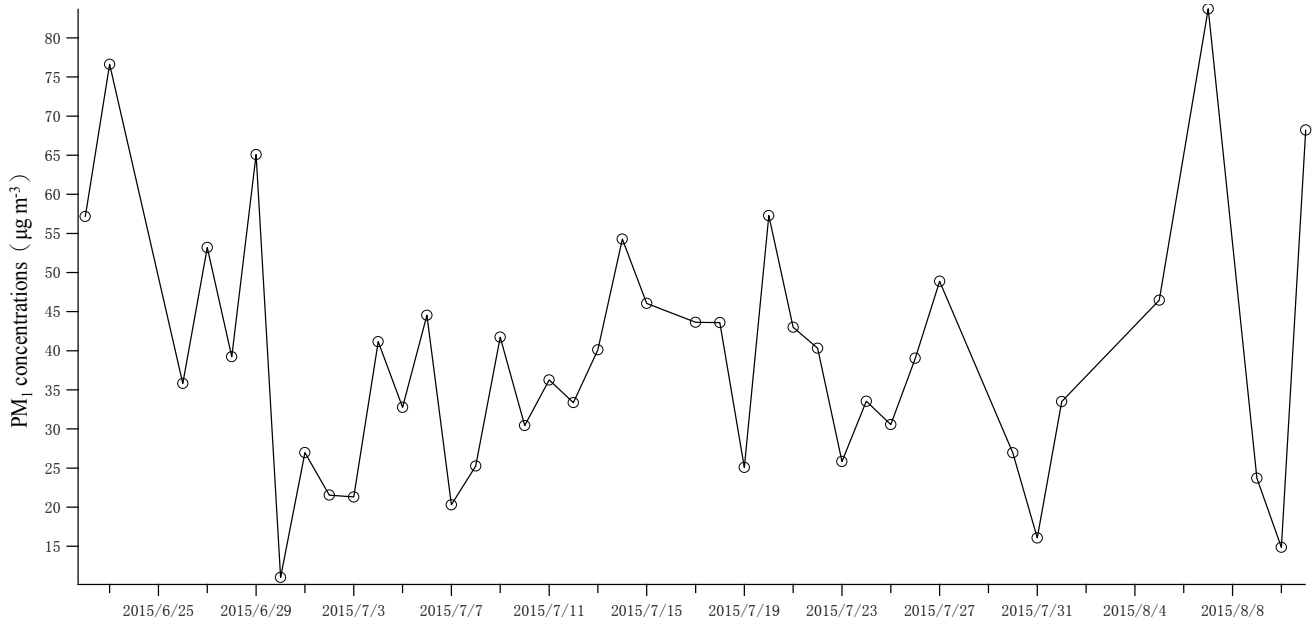

Fig. 2. Time series of PM_1 concentrations on Mount Tai.

Table 1. PM_1 concentrations at different locations (μg m^{-3}).

Locations	Type	Period	PM_1	References
Mount Tai, China	Background	Summer 2015	38.98	This study
Mount Tai, China	Background	Summer 2014	38.16	Zhao *et al.* (2017)
Bologna, Italy	Suburban-farming	Summer 2008	15.52	Sarti *et al.* (2015)
Barcelona, Spain	Urban	Summer 2010–2012	22	Van Drooge *et al.* (2014)
Guangzhou, China	Urban	Summer 2009	29.9	Tao *et al.* (2012)
Xi'an, China	Urban	Summer 2010	72.5	Shen *et al.* (2010)
Lucknow, India	Urban	Summer 2012	8.82	Verma *et al.* (2014)
Virolahti, Finland	Background	Summer 2006	4.3	Makkonen *et al.* (2010)
Aspvreten, Sweden	Background	Summer 2006	17	Ferm *et al.* (2008)
Lake Hongze, China	Background	Spring 2011	36.8	Zhu *et al.* (2016)
Mount Wuzhi, China	Background	Spring 2011	10.9	Zhu *et al.* (2016)

detected (Fig. 3). Since they can potentially induce toxic and carcinogenic effects, WHO has established limits for some of these elements (Table 3). Most of the HMs were lower than their recommended levels except As in PM_1 samples collected on June 29 and July 20 (9.4 and 7.8 ng m^{-3}, respectively; Fig. 4). Similarly, in a previous study investigating wet deposition on Mount Tai, the reported high levels of As could be contributed to the widespread coal consumption industries (coal-power plants, coal mining, domestic heating or cooking) in the north of China (Liu *et al.*, 2010).

Sixteen metallic elements were selected to be analyzed further since they were widely reported and their information have been well known (Table 4). Compared with results from other studies, the concentrations observed at Mount Tai were significantly lower than the ones observed in Changji, China (Liu *et al.*, 2017b); Kanpur campus, India (Singh and Gupta, 2016); Ulsan, Korea (Hieu and Lee, 2010), and Algiers, Algeria (Talbi *et al.*, 2018). However, the concentrations of some elements (such as Al, Ca, Fe and Zn) were higher than those in Istanbul, Turkey (Onat *et al.*, 2013), and Mount Cimone (2165 m a.s.l.) and Salento Peninsula, Italy (Marenco *et al.*, 2006; Perrone *et al.*, 2013).

To investigate the extent of metallic element contamination in the air, the geo-accumulation index (Igeo) was calculated (Fig. 5). The contamination levels were classified according to the method proposed by Muller (1969). In this study, Mn, Al, Co and Sr were recognized as uncontaminated level (Igeo < 0); Mo, Fe, Ca, V, Ti and Ni were classified as uncontaminated to moderately contaminated level (0 < Igeo < 1); Cu, Cr, As and Zn were distinguished as moderately to heavily contaminated level (2 < Igeo < 3); Pb and Cd were identified as heavily (3 < Igeo < 4) and extremely contaminated (Igeo > 5) levels, respectively.

The average enrichment factors (EFs) were also estimated to provide a better insight into the atmospheric content of heavy metals on Mount Tai (Fig. 5). The elements could be classified into three groups according to their enrichment factors: non-enriched crustal metals (Al, Sr, Ti, Ca, Fe, V, Mn, Co, Ni, Mo) with EF < 10, moderately enriched metals (Cu, Cr, As, Zn, Pb) with 10 < EF < 100 and anomalously enriched metals (Cd) with EF > 100.

Integrating the information from Igeo and EF analysis, it could be inferred that Mn, Al, Co, Sr Mo, Fe, Ca, V, Ti and Ni in PM_1 were mainly from crustal origin, while Cu, Cr, As, Zn, Pb and Cd contamination were primarily due to anthropogenic contributions.

PM_1 Dependence on Meteorology

Meteorological conditions, such as temperature (T), wind speed (WS) and relative humidity (RH) may influence the pollutant concentration in atmosphere. Higher temperature is related to greater convection movement, leading to faster diffusion rate of PM, and wind speed is closely related to the dilution of atmospheric pollutants (Wang *et al.*, 2017). Previous researches showed that the heterogeneous reactions under high relative humidity played an important role in the production of secondary aerosols, leading to a positive correlation between fine PM levels and relative humidity (Zhang *et al.*, 2015; Batterman *et al.*, 2016). However, due to complicated interactions between different meteorological factors in the atmospheric environment, results of correlation analysis may not directly reflect the quantitative influence of individual meteorological factors on the pollutants' levels (Chen *et al.*, 2017).

In this study, PM_1 and most metallic elements were not significantly correlated with meteorological factors (Table 5), although a clear meteorological influence could be noticed by studying the pollutant behavior during rain events (Fig. 6). PM_1 concentration increased in the early stage of precipitation, which might be attributed to the stronger effect of high RH levels than precipitation itself on particle mass loading (Sisterson *et al.*, 1985). With the precipitation continuing, a clear decreasing of PM_1 was observed in the final stage of the rain events, denoting scavenging transference by rainwater. The total elemental concentration presented a similar trend, dropping from higher levels to lower levels as a consequence of the rain effect.

Air Mass Analysis

The Hybrid Single Particle Lagrangian Integrated Trajectory (HYSPLIT) model (PC Version 4) developed by the National Oceanic and Atmospheric Administration Air Resources Laboratory (NOAA-ARL) was used to track the origin of air masses carrying particles involved in long-distance transport (Draxler and Rolph, 2003). Based on FNL meteorological dataset, 72-h back trajectories were generated every full hour from June 22 to August 11, with a

Table 2. Minimum, maximum and average concentrations of PM_1-bound metals during the campaign at Mount Tai.

	Total	Si	Fe	Al	Ca	Na	Mg	Ti	K	Zn	Cr	P	Pb	Zr
	μg m^{-3}	μg m^{-3}	μg m^{-3}	μg m^{-3}	μg m^{-3}	μg m^{-3}	μg m^{-3}	μg m^{-3}	μg m^{-3}	μg m^{-3}	μg m^{-3}	μg m^{-3}	μg m^{-3}	μg m^{-3}
Min	2.967	0.711	0.299	0.313	0.240	0.264	0.192	0.054	0.053	7.533	5.329	5.761	4.387	1.688
Max	38.420	8.537	9.995	4.820	6.835	3.540	4.794	2.035	0.614	88.496	135.346	38.384	36.960	67.673
Avg	9.182	2.429	1.758	1.236	1.226	0.950	0.915	0.318	0.208	27.923	22.627	16.410	13.227	13.156
	Ba	V	Cu	Sr	Mn	As	Ni	Sn	Sb	Rb	Li	W	Mo	Ce
	ng m^{-3}	ng m^{-3}	ng m^{-3}	ng m^{-3}	ng m^{-3}	ng m^{-3}	ng m^{-3}	ng m^{-3}	ng m^{-3}	ng m^{-3}	ng m^{-3}	ng m^{-3}	ng m^{-3}	ng m^{-3}
Min	2.542	3.051	1.950	0.979	1.064	1.259	0.711	0.315	0.123	0.164	0.146	0.154	0.121	0.071
Max	86.518	30.193	28.110	23.425	9.325	9.370	15.899	7.341	2.499	1.422	1.249	1,562	0.989	1.041
Avg	13.024	7.349	6.701	5.023	4.322	3.401	2.651	1.347	0.806	0.577	0.488	0,385	0.339	0.334
	Co	Bi	La	Cd	Y	Tl	Cs	Th	U	Sc	Sm	Be		
	ng m^{-3}	ng m^{-3}	ng m^{-3}	ng m^{-3}	ng m^{-3}	ng m^{-3}	ng m^{-3}	ng m^{-3}	ng m^{-3}	ng m^{-3}	ng m^{-3}	ng m^{-3}		
Min	0.033	0.044	0.038	0.034	0.035	0.022	0.020	0.015	0.02	0.005	0.004	0.001		
Max	2.691	0.565	0.488	0.401	0.424	0.282	0.226	0.192	0.16	0.157	0.071	0.027		
Avg	0.249	0.192	0.189	0.171	0.153	0.115	0.077	0.063	0.06	0.053	0.021	0.009		

starting height of 1500 m. Fig. 7 shows the back trajectories ending at Mount Tai during the sampling period. Three categories of air masses could be identified from the analysis. Firstly, "N" air masses coming from north, northwest and northeast originated from the continental inland areas of northern China, Russia and Mongolia. They passed over the provinces of Hebei and Shanxi, and the cities of Beijing and Tianjin. Secondly, "E" marine air masses coming from east, originated mostly from the Korean Peninsula and Japan. Finally, "S" air masses coming from south, southeast and southwest, originated from the continental inland areas of southern China and passed over the provinces of Anhui, Jiangsu and Hubei.

As shown in Table 6, the "N" category represented the highest average PM_1 concentrations, accounting for 41% of the total, followed by "E" (31%) and "S" (28%) categories. The "S" group contained the highest average concentrations of Ca, Ti, Fe, Sr and Cd (Table 6), which were 1616.98 ng m^{-3}, 430.87 ng m^{-3}, 2561.13 ng m^{-3}, 5.45 ng m^{-3} and 0.19 ng m^{-3}, respectively. This can be in part explained by the influence of mining, steel industries as well as coal-fired power plants, which are widely distributed in the southern areas (Liu *et al.*, 2012) and can be related to the presence of a large variety of trace elements in the atmosphere.

Al, Cr, Mn, Cu, Zn, As, Mo and Pb concentrations were found to be higher under "N" category, with average levels of 1361.44 ng m^{-3}, 24.82 ng m^{-3}, 4.85 ng m^{-3}, 7.27 ng m^{-3}, 31.49 ng m^{-3}, 3.62 ng m^{-3}, 0.38 ng m^{-3} and 15.01 ng m^{-3}, respectively. Zn and Pb, as markers of road traffic (Chakraborty and Gupta, 2010; Lin *et al.*, 2015), indicate the influences of air masses passing over the cities of Beijing and Tianjin, where the vehicle population amounted to 4.63 and 1.75 million in 2010, respectively (Lang *et al.*, 2012). As in the environment may be in part due to the presence of coal mining activities like the ones placed in Shanxi and Hebei Provinces. Moreover, since coal combustion is the major energy source in most cities in China, As sources are widely distributed throughout the territory and the average As concentrations did not show significant difference in the three categories. Cr and Cu can be released from coal combustion activities or metallurgical industries placed in the northern provinces (Hussain *et al.*, 2015).

The "E" category contained the lowest levels of total metals but with relatively high concentrations of V, Co and Ni (8.18 ng m^{-3}, 0.46 ng m^{-3} and 3.34 ng m^{-3}, respectively). Ship emissions can contribute to the composition of these air masses leading to higher concentrations of metals such as V, Ni and Co (Ledoux *et al.*, 2017).

Source Analysis

An inter-correlation analysis between 16 selected PM_1-bound elements was conducted and Pearson's correlation coefficients were summarized in Table 7. Positive relationships were found between many groups of elements, among which the strongest correlations (r > 0.9) were found to be: Fe-Ti-Ca, Cu-V-As-Mo, Ni-Co, Pb-Zn-Mo. These results suggested a similar geochemical behavior or

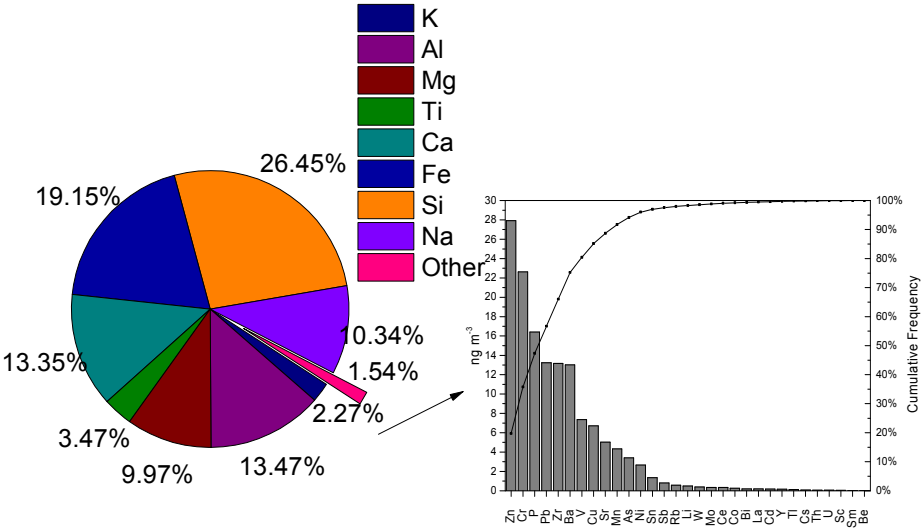

Fig. 3. Elemental composition of PM_1 on Mount Tai.

Table 3. WHO guidelines for heavy metal compounds (ng m^{-3}).

Pb	V	As	Mn	Ni	Cr(VI)	Cd
500	1000	6.6	150	25	0.25	5

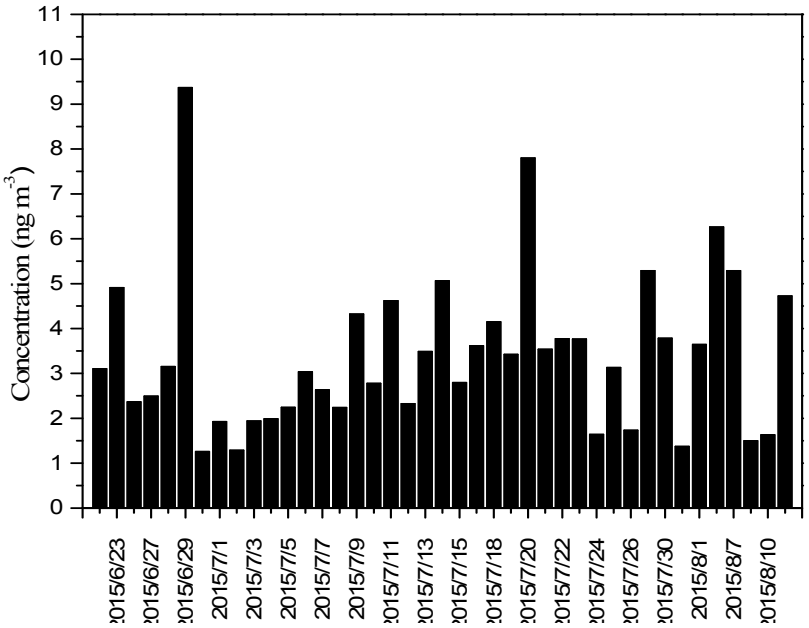

Fig. 4. Time series of As concentrations during the sampling period at Mount Tai.

Table 4. PM_1-bound metallic element concentrations at different locations (ng m^{-3}).

	Al	Sr	Ti	Ca	Fe	V	Cr	Mn	Co	Ni	Cu	Zn	As	Mo	Cd	Pb
Mount Tai, China	1236.5	5	318.3	1226.2	1757.9	7.3	22.6	4.3	0.2	2.7	6.7	27.9	3.4	0.3	0.2	13.2
Changji, China	-	-	-	-	7868.7	125.3	92.1	143.4	6.5	19.4	28.1	-	1210.1	10.7	3	184.1
Istanbul, Turkey	393.3	10.8	13.9	293.7	27.5	0.2	5.9	1.9	0.4	-	3.7	108.2	0.7	0.1	-	-
Mount Cimone, Italy	10.6	-	-	0.9	8.5	-	-	-	-	-	-	0.6	-	-	-	0.2
Ulsan, Korea	163.9	-	-	572.4	255.2	-	8.5	16.5	-	3.8	26.9	116.3	-	-	4	90.1
Salento Peninsula, Italy	70	-	-	-	60	3	4	1	-	3	2	-	-	0.4	0.1	4
Algiers, Algeria	-	426.1	-	3540.2	3293.8	-	19.8	2061.1	-	-	1230.9	-	54.7	28.9	-	204.2
Kanpur, India	-	-	-	-	5760	-	160	150	-	110	330	960	-	-	63	410

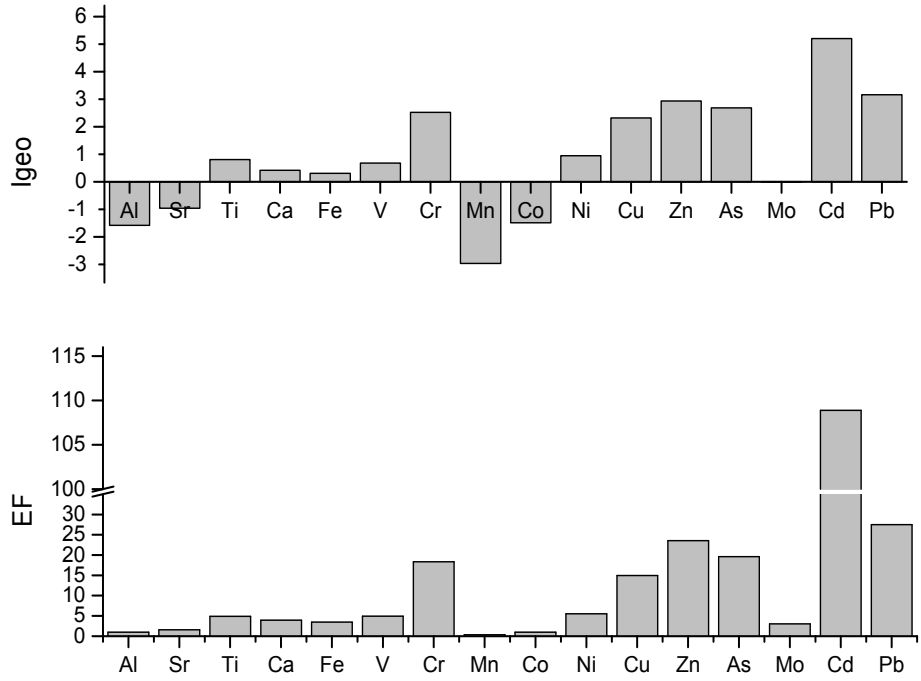

Fig. 5. Average Igeo and EF values calculated for PM_1-bound metallic elements.

Table 5. Pearson correlation coefficients between HM concentrations in PM_1 and meteorological parameters, and air pollutants.

	Al	Sr	Ti	Ca	Fe	V	Cr	Mn	Co	Ni	Cu	Zn	As	Mo	Cd	Pb	PM_1
T	–0.05	–0.12	–0.26	–0.06	–0.24	–0.22	–0.20	0.04	–0.17	–0.19	–0.28	–0.24	–0.08	–0.21	0.13	–0.24	0.04
RH	0.20	0.03	0.01	0.12	0.03	0.22	0.05	**–0.75****	0.08	0.17	–0.05	–0.12	0.24	0.04	**–0.42****	0.00	0.14
WS	–0.14	0.02	0.05	0.00	0.05	–0.16	0.01	**0.77****	0.02	–0.05	0.10	0.15	–0.23	–0.03	0.32	0.05	–0.18

T: Average Temperature (°C). RH: Average relative humidity (%). WS: Average wind speed (km h^{-1}).
** Correlation is significant at the 0.01 level (2-tailed).

common sources of these metals (Olatunde, 2015). In order to identify them, PCA was applied to group the elements in main source categories and the results are shown in Fig. 8.

Three factors accounted for 81.4% of the total variance. Factor 1, explaining 46.20% of the variance, showed high loading for Cr, Cu and As. Metal processing industries placed in southern and northern China, fuel oil and coal combustion can be partly responsible for Cr and Cu emissions (Liu *et al.*, 2012; Doushanov, 2015). As represents a marker of coal combustion (Tan *et al.*, 2017) and coal mining. For these reasons, Factor 1 included coal burning, coal mining and metallurgic activities.

Factor 2, explaining 21.50% of the variance, included Mn, Cd, Zn and Pb. Among them, Zn and Pb showed a strong correlation (r = 0.92, p < 0.01). Ratio of Pb/Zn between 0.23 and 33.3 indicate possible sources from automotive emissions (Arditsoglou and Samara, 2005). In this study, the average Pb/Zn ratio (calculated as the slope of a linear regression line with R^2 = 0.81) was 0.45, very close to those measured from $PM_{2.5}$ in Fukuoka, Japan, and TSP in Beijing, China (0.44 and 0.43, respectively) (Kaneyasu *et al.*, 2014). Similar to Pb and Zn, Mn and Cd can be originated from vehicle exhaust for the use of fuel additives and lubricating oil additives (Duan and Tan, 2013). Therefore, we identified Factor 2 as the traffic source.

Factor 3, explaining 13.74% of the variance, was dominated by the elements Co and Ni. These elements exhibited higher levels in the marine air masses coming from east. In previous studies, Co and Ni were related to ship emissions (Ledoux *et al.*, 2017). According to the results from Igeo and EF analysis (Section 3.1), Co was classified as a crustal element, while Ni was linked to both crustal and anthropogenic sources. Hence, this factor can be attributed to the presence of relative clean marine air masses.

Heavy Metals Risk Assessment

It is well known that some HMs can lead to adverse consequences on human body. For example, IARC has classified Cd as Group 1 human carcinogens since they can induce lung cancers in humans and animals exposed by inhalation (WHO, 2006). Metallic Ni has also been classified as possibly carcinogenic to humans, and vanadium exposure of Ni can lead to acute and chronic effects on the respiratory system (Kiviluoto *et al.*, 1979; Lees, 1980; WHO, 2006). Many researches have been conducted on health risk assessment of metals in urban sites and industrial areas (Huang *et al.*, 2014; Lin *et al.*, 2015; Zheng *et al.*, 2015). In this study, making use of the background HM

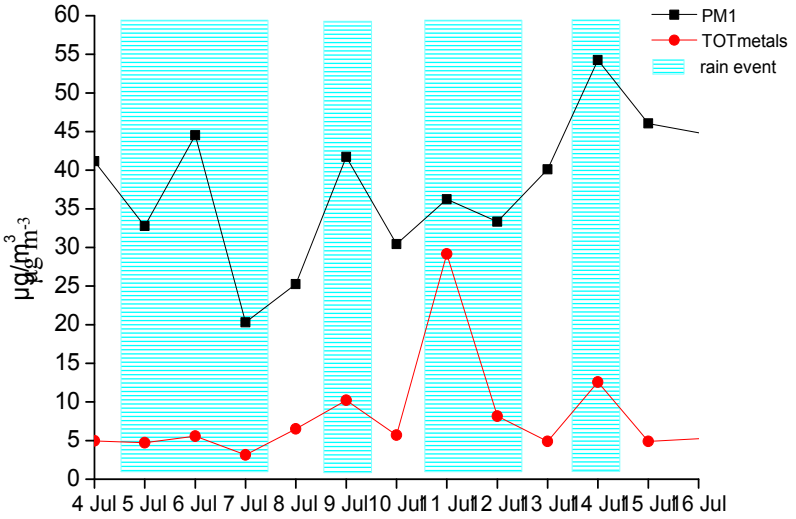

Fig. 6. Total metal content and PM_1 timeline from July 4 to July 16.

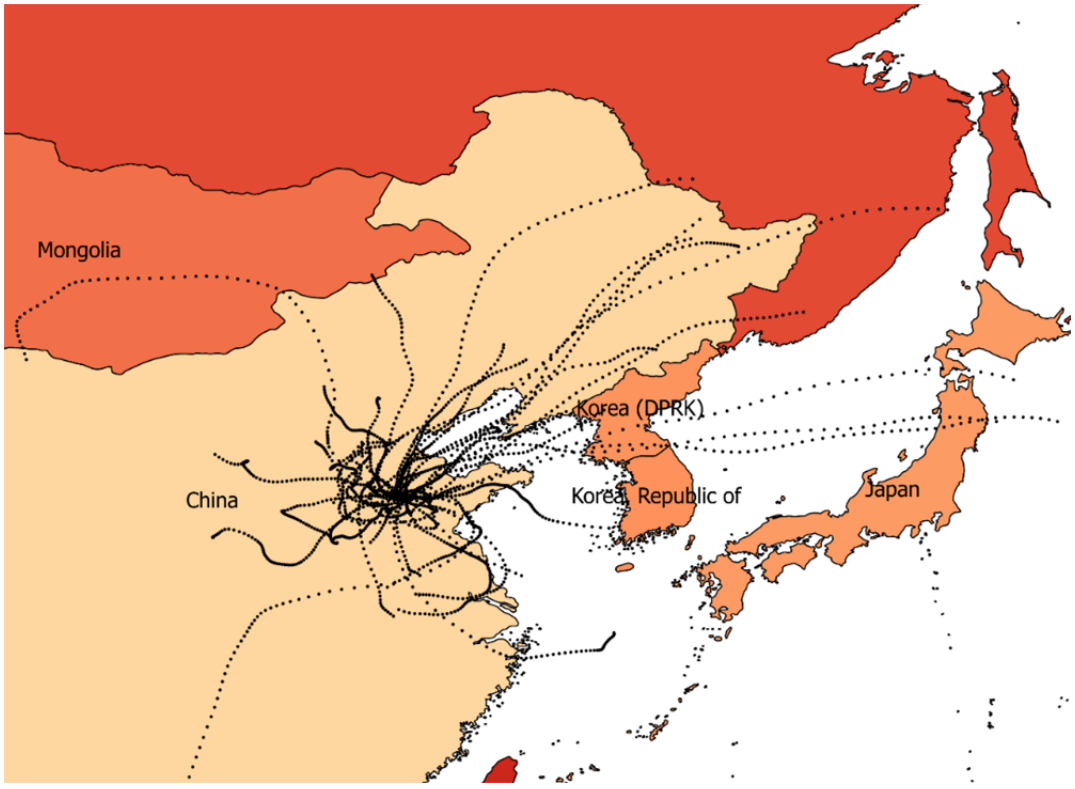

Fig. 7. Back trajectories of the air masses arriving at Mount Tai from June 22 to August 11.

concentrations at Mount Tai, we evaluated the baseline of inhalation exposure values for public health. The health risks posed by PM_1-bound heavy metals were evaluated using the method described by Liu *et al.* (2017b), with reference to four population categories: elderly, males, females and children.

Based on the health concern posed by different elements, two categories were created: "A" category, including Al, Sr, Ti, Ca and Fe; "B" category, including V, Cr, Ni, Cu, Zn, As, Mo, Cd, Pb, Mn and Co. For the elements constituting the "A" category, RfD values for inhalation exposure pathway have not been established by USEPA. Thus, we only assessed the risk induced by the elements in "B" category. The toxicity values used in the analysis and the average daily exposure parameters were summarized in Table 8 (Izhar *et al.*, 2016; Singh and Gupta, 2016; Liu *et al.*, 2017b) and Table 9 (Liu *et al.*, 2017b), respectively. Table 10 shows the average daily exposure doses, the non-carcinogenic (HQ) and the carcinogenic (ILCR) risks derived from the inhalation exposure.

Among the nine heavy metals, the highest non-carcinogenic risk of inhalation (HQ) appeared to occur for

Table 6. Mean concentrations of PM_1 and PM_1-bound metals at Mount Tai under different air masses.

	PM_1 μg m^{-3}	Tot metals μg m^{-3}	Al ng m^{-3}	Sr ng m^{-3}	Ti ng m^{-3}	Ca ng m^{-3}	Fe ng m^{-3}	V ng m^{-3}	Cr ng m^{-3}	Mn ng m^{-3}	Co ng m^{-3}	Ni ng m^{-3}	Cu ng m^{-3}	Zn ng m^{-3}	As ng m^{-3}	Mo ng m^{-3}	Cd ng m^{-3}	Pb ng m^{-3}
N	44.70	9.00	1361.44	5.18	257.02	1059.23	1463.75	7.62	24.82	4.85	0.23	2.80	7.27	31.49	3.62	0.38	0.18	15.01
E	34.14	8.51	1191.88	3.75	360.00	1133.09	1465.35	8.18	17.43	2.84	0.46	3.34	5.33	19.82	3.51	0.26	0.11	9.97
S	31.15	10.39	1142.57	5.45	430.87	1616.98	2561.13	6.82	24.43	4.31	0.15	2.00	6.89	26.50	3.04	0.32	0.19	12.35

Table 7. Pearson's correlation matrix for the concentrations of heavy metals in PM_1 collected on Mount Tai. Values between 0.5 and 0.8 are in bold and values higher than 0.8 are in bold and underlined.

	Al	Sr	Ti	Ca	Fe	V	Cr	Mn	Co	Ni	Cu	Zn	As	Mo	Cd
Sr	**0.71****														
Ti	**0.68****	**0.65****													
Ca	**0.59****	**0.66****	**0.68****												
Fe	**0.63****	**0.62****	**0.93****	**0.81****											
V	**0.79****	**0.76****	**0.77****	**0.62****	**0.70****										
Cr	**0.58****	**0.59****	**0.70****	0.47**	**0.62****	**0.78****									
Mn	0.12	0.24	0.13	0.11	0.14	0.18	0.19								
Co	0.21	0.27	–0.06	0.10	–0.06	0.15	0.01	0.20							
Ni	0.41**	**0.51****	0.15	0.25	0.13	0.41**	0.25	0.19	**0.90****						
Cu	**0.68****	**0.76****	**0.76****	**0.55****	**0.72****	**0.88****	**0.75****	0.49**	0.16	0.39*					
Zn	0.45**	**0.57****	0.48**	0.36*	0.41**	**0.69****	**0.62****	**0.62****	0.08	0.28	**0.81****				
As	**0.73****	**0.71****	**0.65****	**0.60****	**0.61****	**0.94****	**0.69****	0.22	0.13	0.36*	**0.82****	**0.72****			
Mo	**0.58****	**0.68****	**0.59****	**0.50****	**0.57****	**0.82****	**0.77****	0.46**	0.06	0.28	**0.90****	**0.86****	**0.82****		
Cd	–0.18	–0.06	–0.12	–0.13	–0.13	–0.03	0.00	**0.55****	–0.07	–0.04	0.19	**0.52****	0.11	0.28	
Pb	0.44**	**0.51****	0.45**	0.41**	0.43**	**0.66****	**0.58****	**0.55****	0.14	0.33*	**0.74****	**0.92****	**0.72****	**0.81****	0.48**

** Correlation is significant at the 0.01 level (2-tailed).

* Correlation is significant at the 0.05 level (2-tailed).

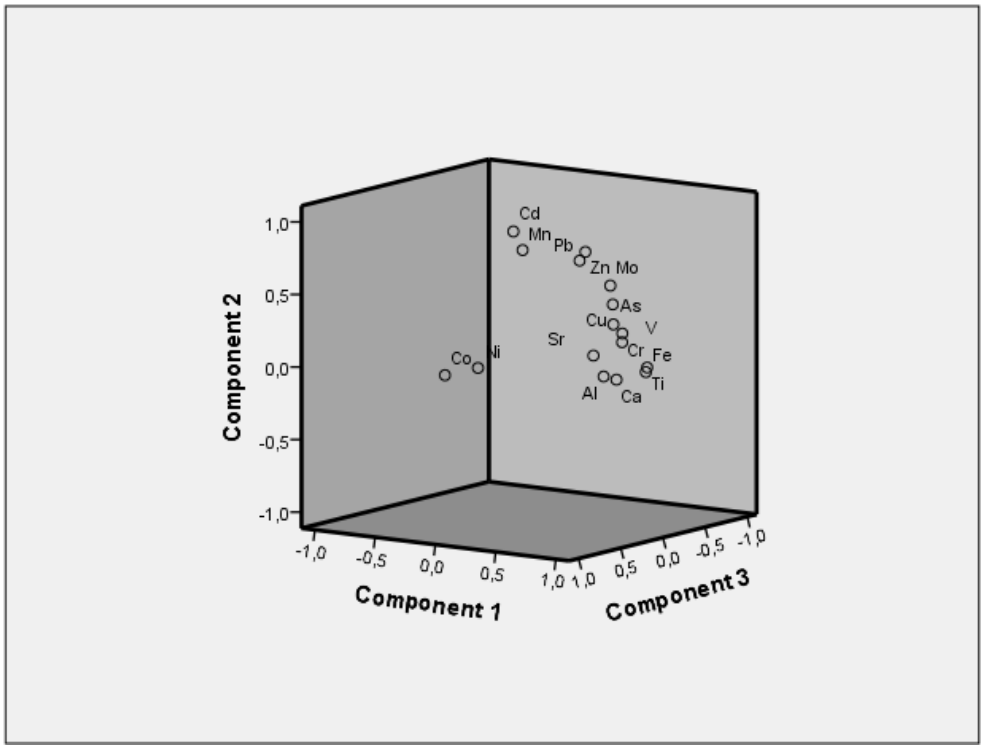

Fig. 8. Component plot in rotated space (with varimax rotation) for PM_1-bound heavy metals detected on Mount Tai.

Table 8. Toxicity values used in this study.

Heavy metals	V	Cr	Ni	Cu	Zn	As	Mo	Cd	Pb	Mn	Co
Inhal. RfD (mg kg^{-1} d^{-1})	5.00E-03	2.86E-05	3.52E-03	4.00E-02	3.00E-01	3.00E-04	5.00E-03	1.00E-03	3.52E-03	1.43E-05	5.70E-06
Inhal. SF (kg d mg^{-1})	-	42	0.84	-	-	15.1	-	6.3	-	-	9.8

Table 9. Values of daily exposure parameters used in the risk assessment of HMs.

Parameters	Elderly	Males	Females	Children
RR	13.7	119.02	14.17	7.5
Ef	365	365	365	365
ED	70	30	30	6
BW	50.8	62.7	54.4	15
AT	70 × 365	30 × 365	30 × 365	6 × 365

Cr, ranging between 2.06E-01 (for females) and 3.95E-01 (for children). However, HQ values were all less than 1, suggesting that non-carcinogenic effects were unlikely to occur. For all the population groups, Mo and Zn posed the lowest risk levels among the nine elements.

The hazard index (HI) was calculated for each category as the sum of the HQs for the metals, representing the total risk of non-carcinogenic effects for multiple elements (Singh and Gupta, 2016). The HI values were 0.31, 0.35, 0.30, 0.57 for elderly, males, females and children, respectively, which did not exceed the safe limit (HI < 1).

Incremental lifetime cancer risk (ILCR) was calculated for Cd, Ni, As, Cr and Co which have been known for their carcinogenic potential according to the International Agency for Research on Cancer (IARC) (IARC, 2007). Since Cr (VI), different from the other forms of Cr, was classified as Group 1, the concentration of Cr(VI) used for the carcinogenic risk assessment was calculated as one-seventh of the total Cr concentration (Hieu and Lee, 2010). According to the USEPA, an increase of one incidence of cancer per million people, corresponding to an ILCR value > 10^{-6}, represents the baseline value of acceptable risk. In this study, ILCR values of single elements ranged from 3.28 E-07 to 6.78E-05, and those of Cr, As and Ni exceeded the reference value. The total ILCRs were 10 times higher than the thresholds for all the population categories, suggesting the potential cancer risk for general population. Particularly, the female category was the least susceptible to both non-carcinogenic and carcinogenic risks induced by PM_1-bound HMs, while the children's group was the most vulnerable.

Table 10. Risk analysis results.

	V	Cr	Ni	Cu	Zn	As	Mo	Cd	Pb	Mn	Co	Total
ADDinh elderly	1.97E-06	6.09E-06	7.28E-07	1.81E-06	7.52E-06	9.17E-07	8.09E-08	5.39E-08	3.56E-06	1.16E-06	5.39E-08	2.39E-05
ADDinh male	2.21E-06	6.86E-06	8.19E-07	2.03E-06	8.46E-06	1.03E-06	9.10E-08	6.07E-08	4.00E-06	1.30E-06	6.07E-08	2.69E-05
ADDinh female	1.90E-06	5.89E-06	7.03E-07	1.75E-06	7.27E-06	8.86E-07	7.81E-08	5.21E-08	3.44E-06	1.12E-06	5.21E-08	2.31E-05
ADDinh children	3.65E-06	1.13E-05	1.35E-06	3.35E-06	1.40E-05	1.70E-06	1.50E-07	1.00E-07	6.60E-06	2.15E-06	1.00E-07	4.45E-05
HQ elderly	3.94E-04	2.13E-01	2.07E-04	4.52E-05	2.51E-05	3.06E-03	1.62E-05	5.39E-05	1.01E-03	8.11E-02	9.46E-03	3.08E-01
HQ male	4.43E-04	2.40E-01	2.33E-04	5.08E-05	2.82E-05	3.44E-03	1.82E-05	6.07E-05	1.14E-03	9.12E-02	1.06E-02	3.47E-01
HQ female	3.80E-04	2.06E-01	2.00E-04	4.36E-05	2.42E-05	2.95E-03	1.56E-05	5.21E-05	9.77E-04	7.83E-02	9.14E-03	2.98E-01
HQ children	7.30E-04	3.95E-01	3.84E-04	8.38E-05	4.65E-05	5.67E-03	3.00E-05	1.00E-04	1.88E-03	1.50E-01	1.75E-02	5.71E-01
ILCR elderly	-	3.66E-05	6.12E-07	-	-	1.38E-05	-	3.40E-07	-	-	5.29E-07	5.19E-05
ILCR male	-	4.11E-05	6.88E-07	-	-	1.56E-05	-	3.82E-07	-	-	5.95E-07	5.84E-05
ILCR female	-	3.53E-05	5.91E-07	-	-	1.34E-05	-	3.28E-07	-	-	5.11E-07	5.01E-05
ILCR children	-	6.78E-05	1.13E-06	-	-	2.57E-05	-	6.30E-07	-	-	9.80E-07	9.62E-05

ADD_{inh}: Average daily exposure doses (mg kg^{-1} d^{-1}).
HQ: Hazard quotient.
ILCR: incremental lifetime cancer risk.

CONCLUSIONS

Daily PM_1 samples, which ranged in concentration from 11.02 to 83.71 μg m^{-3}, with an average of 38.98 μg m^{-3}, were collected at a high mountain site in northern China during a summer campaign (June 2015–August 2015). The PM-bound metallic elements were analyzed, and their characteristics were investigated. Of the metallic elements, Cd, Pb, Zn, As, Cr and Cu showed higher EF and Igeo values, with average concentrations of 0.17 ng m^{-3}, 13.23 ng m^{-3}, 27.92 ng m^{-3}, 3.40 ng m^{-3}, 22.63 ng m^{-3} and 1.226 ng m^{-3}, respectively. Back trajectory analysis was conducted to determine the influence of different air mass categories. Air masses coming from the northern parts of China displayed the highest average PM_1 concentration, whereas those originating in the south and the east had the highest and the lowest total elemental concentrations, respectively. Results obtained from PCA analysis indicated that the PM_1-bound heavy metal compounds originated in multiple sources, including coal combustion, metallurgic activities and vehicle and ship emission. Using the background HM concentrations at Mount Tai, the baseline of the inhalation exposure risk to public health was assessed. The results indicated that non-carcinogenic effects due to the inhalation of heavy metals were unlikely to occur for all population groups (the elderly, males, females and children). By contrast, the total ILCR values were about 10 times higher than the reference value of 1×10^{-6}, indicating a potential health risk to the general population.

ACKNOWLEDGMENTS

We acknowledge the Mount Tai Meteorological Station for their support on the field study. We appreciate the help of sample collecting and analysis from Tao Li, Fan Xiao, Yun-jun Jiang, Xiao-biao Guo. Financial supports were provided by National Natural Science Foundation of China (41601548, 81602827, 41573107), Tianjin Municipal Education Commission Research Project (2017KJ244), Training Program for Innovative Research Team in Tianjin Institutions of Higher Education (TD13-5021), Wuqing District Science and technology development program (WQKJ201614) and Tianjin 131 innovative talent training project.

REFERENCES

Arditsoglou, A. and Samara, C. (2005). Levels of total suspended particulate matter and major trace elements in Kosovo: S source identification and apportionment study. *Chemosphere* 59: 669–678.

Aurela, M., Saarikoski, S., Niemi, J.V., Canonaco, F., Prevot, A.S.H., Frey, A., Carbone, S., Kousa, A. and Hillamo, R. (2015). Chemical and source characterization of submicron particles at residential and traffic sites in the Helsinki metropolitan area, Finland. *Aerosol Air Qual. Res.* 15: 1213–1226.

Batterman, S., Xu, L., Chen, F., Chen, F. and Zhong, X. (2016). Characteristics of $PM_{2.5}$ concentrations across

Beijing during 2013–2015. *Atmos. Environ.* 145: 104–114.

Blanco-Becerra, L.C., Gáfaro-Rojas, A.I. and Rojas-Roa, N.Y. (2015). Influence of precipitation scavenging on the $PM_{2.5}/PM_{10}$ ratio at the Kennedy locality of Bogotá, Colombia. *Rev. Fac. Ing. Univ. Ant.* 76: 58–65.

Chakraborty, A. and Gupta, T. (2010). Chemical characterization and source apportionment of submicron (PM_1) aerosol in Kanpur region, India. *Aerosol Air Qual. Res.* 10: 433–445.

Chen, G., Knibbs, L.D., Zhang, W., Li, S., Cao, W., Guo, J., Ren, H., Wang, B., Wang, H. and Williams, G. (2017). Estimating spatiotemporal distribution of PM_1 concentrations in China with satellite remote sensing, meteorology, and land use information. *Environ. Pollut.* 233: 1086–1094.

Doushanov, D. (2015). Control of pollution in the iron and steel industry. Pollution Control Technologies – Vol. III - Control of Pollution in the Iron and Steel Industry, Encyclopedia of Life Support Systems (EOLSS), Abu Dhabi, United Arab Emirates.

Draxler, R. and Rolph, G. (2003). HYSPLIT (HYbrid Single-Particle Lagrangian Integrated Trajectory). NOAA Air Resources Laboratory, Silver Spring, MD. Model access via NOAA ARL READY Website.

Duan, J. and Tan, J. (2013). Atmospheric heavy metals and arsenic in China: Situation, sources and control policies. *Atmos. Environ.* 74: 93–101.

Galindo, N., Yubero, E., Nicolas, J.F., Crespo, J. and Soler, R. (2016). Chemical characterization of PM_1 at a regional background site in the Western Mediterranean. *Aerosol Air Qual. Res.* 16: 530–541.

Harrison, R.M., Jones, A.M. and Lawrence, R.G. (2004). Major component composition of PM_{10} and $PM_{2.5}$ from roadside and urban background sites. *Atmos. Environ.* 38: 4531–4538.

Hieu, N.T. and Lee, B.K. (2010). Characteristics of particulate matter and metals in the ambient air from a residential area in the largest industrial city in Korea. *Atmos. Res.* 98: 526–537.

Huang, M., Wang, W., Chan, C.Y., Cheung, K.C., Man, Y.B., Wang, X. and Wong, M.H. (2014). Contamination and risk assessment (based on bioaccessibility via ingestion and inhalation) of metal(loid)s in outdoor and indoor particles from urban centers of Guangzhou, China. *Sci. Total Environ.* 479: 117–124.

Huang, X. (2013). *$PM_{2.5}$: The contribution of coal burning to air pollution in Beijing.* Master Thesis, Department of Earth Sciences, Uppsala University, Uppsala, Sweden.

Hussain, K., Rahman, M., Prakash, A. and Hoque, R.R. (2015). Street dust bound PAHs, carbon and heavy metals in Guwahati city – Seasonality, toxicity and sources. *Sustainable Cities Soc.* 19: 17–25.

IARC (International Agency for Research on Cancer) (2007). Combined Estrogen-Progestogen contraceptives and combined Estrogen-Progestogen menopausal therapy. IARC monographs on the evaluation of carcinogenic risks to humans. IARC Monographs, Volume 91, International Agency for Research on Cancer, Lyon, France.

Izhar, S., Goel, A., Chakraborty, A. and Gupta, T. (2016). Annual trends in occurrence of submicron particles in ambient air and health risk posed by particle bound metals. *Chemosphere* 146: 582–590.

Kaneyasu, N., Yamamoto, S., Sato, K., Takami, A., Hayashi, M., Hara, K., Kawamoto, K., Okuda, T. and Hatakeyama, S. (2014). Impact of long-range transport of aerosols on the $PM_{2.5}$ composition at a major metropolitan area in the northern Kyushu area of Japan. *Atmos. Environ.* 97: 416–425.

Khan, M.F., Hirano, K. and Masunaga, S. (2012). Assessment of the sources of suspended particulate matter aerosol using US EPA PMF3.0. *Environ. Monit. Assess.* 184: 1063–1083.

Kiviluoto, M., Räsänen, O., Rinne, A. and Rissanen, M. (1979). Effects of vanadium on the upper respiratory tract of workers in a vanadium factory: A macroscopic and microscopic study. *Scand. J. Work Environ. Health* 5: 50–58.

Kozakova, J., Pokorna, P., Cernikova, A., Hovorka, J., Branis, M., Moravec, P. and Schwarz, J. (2017). The association between intermodal ($PM_{1\text{-}2.5}$) and PM_1, $PM_{2.5}$, coarse fraction and meteorological parameters in various environments in central Europe. *Aerosol Air Qual. Res.* 17: 1234–1243.

Křůmal, K., Mikuška, P. and Večeřa, Z. (2017). Characterization of organic compounds in winter PM_1 aerosols in a small industrial town. *Atmos. Pollut. Res.* 8: 930–939.

Lang, J., Cheng, S., Wei, W., Zhou, Y., Wei, X. and Chen, D. (2012). A study on the trends of vehicular emissions in the Beijing–Tianjin–Hebei (BTH) region, China. *Atmos. Environ.* 62: 605–614.

Ledoux, F., Kfoury, A., Delmaire, G., Roussel, G., El Zein, A. and Courcot, D. (2017). Contributions of local and regional anthropogenic sources of metals in $PM_{2.5}$ at an urban site in northern France. *Chemosphere* 181: 713–724.

Lees, R. (1980). Changes in lung function after exposure to vanadium compounds in fuel oil ash. *Occup. Environ. Med.* 37: 253–256.

Li, H., Wang, Q.G., Yang, M., Li, F., Wang, J., Sun, Y., Wang, C., Wu, H. and Qian, X. (2016). Chemical characterization and source apportionment of $PM_{2.5}$ aerosols in a megacity of Southeast China. *Atmos. Res.* 181: 288–299.

Li, P.H., Wang, Y., Li, Y.H., Wang, Z.H., Zhang, H.Y., Xu, P.J. and Wang, W.X. (2010). Characterization of polycyclic aromatic hydrocarbons deposition in $PM_{2.5}$ and cloud/fog water at Mount Taishan (China). *Atmos. Environ.* 44: 1996–2003.

Li, P.H., Kong, S.F., Geng, C.M., Han, B., Lu, B., Sun, R.F., Zhao, R.J. and Bai, Z.P. (2013). Assessing the hazardous risks of vehicle inspection workers' exposure to particulate heavy metals in their work places. *Aerosol Air Qual. Res.* 13: 255–265.

Lin, C.C., Tsai, J.H., Huang, K.L., Yeh, C.K.J., Chen, H.L., Chen, S.J., Lee, J.T. and Hsieh, Y.C. (2016). Characteristics of respirable particulate metals emitted by a beehive firework display in YanShuei area of southern

Taiwan. *Aerosol Air Qual. Res.* 16: 2227–2236.

Lin, Y.C., Tsai, C.J., Wu, Y.C., Zhang, R., Chi, K.H., Huang, Y.T., Lin, S.H. and Hsu, S.C. (2015). Characteristics of trace metals in traffic-derived particles in Hsuehshan Tunnel, Taiwan: Size distribution, potential source, and fingerprinting metal ratio. *Atmos. Chem. Phys.* 15: 4117–4130.

Liu, J., Wang, Y., Li, P.H., Shou, Y.P., Li, T., Yang, M.M., Wang, L., Yue, J.J., Yi, X.L. and Guo, L.Q. (2017a). Polycyclic aromatic hydrocarbons (PAHs) at high mountain site in North China: Concentration, source and health risk assessment. *Aerosol Air Qual. Res.* 17: 2867–2877.

Liu, X.H., Wai, K.M., Wang, Y., Zhou, J., Li, P.H., Guo, J., Xu, P.J. and Wang, W.X. (2012). Evaluation of trace elements contamination in cloud/fog water at an elevated mountain site in Northern China. *Chemosphere* 88: 531–541.

Liu, Y.Y., Shen, Y.X., Liu, C. and Liu, H.F. (2017b). Enrichment and assessment of the health risks posed by heavy metals in PM_1 in Changji, Xinjiang, China. *J. Environ. Sci. Health A* 52: 413–419.

Majewski, G., Rogula-Kozlowska, W., Rozbicka, K., Rogula-Kopiec, P., Mathews, B. and Brandyk, A. (2018). Concentration, chemical composition and origin of PM_1: Results from the first long-term measurement campaign in Warsaw (Poland). *Aerosol Air Qual. Res.* 18: 636–654.

Marenco, F., Bonasoni, P., Calzolari, F., Ceriani, M., Chiari, M., Cristofanelli, P., D'Alessandro, A., Fermo, P., Lucarelli, F. and Mazzei, F. (2006). Characterization of atmospheric aerosols at Monte Cimone, Italy, during summer 2004: Source apportionment and transport mechanisms. *J. Geophys. Res.* 111: D24202.

Motallebi, N., Tran, H., Croes, B.E. and Larsen, L.C. (2003). Day-of-week patterns of particulate matter and its chemical components at selected sites in California. *J. Air Waste Manage. Assoc.* 53: 876–888.

Muller, G. (1969). Index of geoaccumulation in sediments of the Rhine River. *GeoJournal* 2: 108–118.

Odat, S. (2015). Application of Geoaccumulation Index and Enrichment Factors on the Assessment of Heavy Metal Pollution along Irbid/zarqa Highway-Jordan. *J. Appl. Sci.* 15: 1318–1321.

Olatunde, P.S. (2015). Geochemical and statistical approach to assessing trace metal accumulations in Lagos Lagoon Sediments, South Western, Nigeria.

Ollier, S. (2013). Indoor and ambient particulate matter relationships during the heating season. Report, Department of Geophysics, Faculty of Science, University of Zagreb 36.

Onat, B., Sahin, U.A. and Akyuz, T. (2013). Elemental characterization of $PM_{2.5}$ and PM_1 in dense traffic area in Istanbul, Turkey. *Atmos. Pollut. Res.* 4: 101–105.

Pacyna, J.M. and Pacyna, E.G. (2001). An assessment of global and regional emissions of trace metals to the atmosphere from anthropogenic sources worldwide. *Environ. Rev.* 9: 269–298.

Papaoikonomou, K., Emmanouil, C., Vasilatou, V., Diapouli, E., Grigoratos, T., Zafirakou, A. and Kungolos, A. (2018). PM_{10} and elemental concentrations in a dismantling plant for waste of electrical and electronic equipment in Greece. *Aerosol Air Qual. Res.* 18: 1457–1469.

Perrone, M., Becagli, S., Orza, J.G., Vecchi, R., Dinoi, A., Udisti, R. and Cabello, M. (2013). The impact of long-range-transport on PM_1 and $PM_{2.5}$ at a Central Mediterranean site. *Atmos. Environ.* 71: 176–186.

Prodi, F. and Tampieri, F. (1982). The removal of particulate matter from the atmosphere: The physical mechanisms. *Pure Appl. Geophys.* 120: 286–325.

Radulescu, C., Iordache, S., Dunea, D., Stihi, C. and Dulama, I.D. (2015). Risks assessment of heavy metals on public health associated with atmospheric exposure to $PM_{2.5}$ in urban area. *Rom. J. Phys.* 60: 1171–1182.

Singh, D.K. and Gupta, T. (2016). Source apportionment and risk assessment of PM, bound trace metals collected during foggy and non-foggy episodes at a representative site in the Indo-Gangetic plain. *Sci. Total Environ.* 550: 80–94.

Sisterson, D., Johnson, S. and Kumar, R. (1985). The influence of humidity on fine-particle aerosol dynamics and precipitation scavenging. *Aerosol Sci. Technol.* 4: 287–300.

Stallins, J.A., Carpenter, J., Bentley, M.L., Ashley, W.S. and Mulholland, J.A. (2013). Weekend-weekday aerosols and geographic variability in cloud-to-ground lightning for the urban region of Atlanta, Georgia, USA. *Reg. Environ. Change* 13: 137–151.

Talbi, A., Kerchich, Y., Kerbachi, R. and Boughedaoui, M. (2018). Assessment of annual air pollution levels with PM_1, $PM_{2.5}$, PM_{10} and associated heavy metals in Algiers, Algeria. *Environ. Pollut.* 232: 252–263.

Tan, J., Zhang, L., Zhou, X., Duan, J., Li, Y., Hu, J. and He, K. (2017). Chemical characteristics and source apportionment of $PM_{2.5}$ in Lanzhou, China. *Sci. Total Environ.* 601: 1743–1752.

Tian, H., Zhu, C., Gao, J., Cheng, K., Hao, J., Wang, K., Hua, S., Wang, Y. and Zhou, J. (2015). Quantitative assessment of atmospheric emissions of toxic heavy metals from anthropogenic sources in China: Historical trend, spatial distribution, uncertainties, and control policies. *Atmos. Chem. Phys.* 15: 10127–10147.

US EPA (2001). National primary and secondary ambient air quality standard. 40 CFR Part 50.

Ventura, L.M.B., Mateus, V.L., de Almeida, A.C.S.L., Wanderley, K.B., Taira, F.T., Saint'Pierre, T.D. and Gioda, A. (2017). Chemical composition of fine particles ($PM_{2.5}$): Water-soluble organic fraction and trace metals. *Air Qual. Atmos. Health* 10: 845–852.

Wang, J., Ji, H., Wang, Q.Q., Li, H., Qian, X., Li, F. and Yang, M. (2017). Prediction of size-fractionated airborne particle-bound metals using MLR, BP-ANN and SVM analyses. *Chemosphere* 180: 513–522.

Wang, Y., Guo, J., Wang, T., Ding, A., Gao, J., Zhou, Y., Collett, J.L. and Wang, W. (2011). Influence of regional pollution and sandstorms on the chemical composition of cloud/fog at the summit of Mt. Taishan in northern China. *Atmos. Res.* 99: 434–442.

WHO (2006). Air quality guidelines: Global update 2005. Particulate Matter, Ozone, Nitrogen Dioxide and Sulfur Dioxide. World Health Organization, Switzerland.

WHO (2013). Health effects of particulate matter. Policy implications for countries in Eastern Europe. Caucasus and central Asia. World Health Organization Regional Office for Europe, Copenhagen.

Zhai, Y., Liu, X., Chen, H., Xu, B., Zhu, L., Li, C. and Zeng, G. (2014). Source identification and potential ecological risk assessment of heavy metals in $PM_{2.5}$ from Changsha. *Sci. Total Environ.* 493: 109–115.

Zhang, Y., Zhang, X., Zhang, Y., Shen, X., Sun, J., Ma, Q., Yu, X., Zhu, J., Zhang, L. and Che, H. (2015). Significant concentration changes of chemical components of PM_1 in the Yangtze River Delta area of China and the implications for the formation mechanism of heavy haze-fog pollution. *Sci. Total Environ.* 538: 7–15.

Zhao, T., Yang, L., Yan, W., Zhang, J., Lu, W., Yang, Y., Chen, J. and Wang, W. (2017). Chemical characteristics of $PM_1/PM_{2.5}$ and influence on visual range at the summit of Mount Tai, North China. *Sci. Total Environ.* 575: 458–466.

Zheng, X., Zhao, W., Yan, X., Shu, T., Xiong, Q. and Chen, F. (2015). Pollution characteristics and health risk assessment of airborne heavy metals collected from Beijing bus stations. *Int. J. Environ. Res. Public Health* 12: 9658–9671.

Received for review, April 10, 2018
Revised, August 10, 2018
Accepted, August 21, 2018